Stress Gradient Correction Factor for Stress Intensity at Welded Stiffeners and Cover Plates

Correction factor curves are correlated with stress concentration decay from an elliptical hole in a uniaxially stressed plate, thereby providing a means of predicting the correction factor for arbitrary geometries

BY N. ZETTLEMOYER AND J. W. FISHER

Introduction

Fatigue damage at many welded structural details can be primarily attributed to propagation of a crack from an initial flaw or discontinuity at a weld toe.[5,6] The driving force behind such propagation is the fluctuation or range of the stress intensity factor ΔK.[11] The range of stress intensity is often expressed as ΔK for a central, through crack in an infinite plate under uniaxial tension, adjusted by superimposed correction factors.[1,14,16,17]

$$\Delta K = F_s F_w F_e F_g * S_r \sqrt{\pi a} \qquad (1)$$

S_r is the nominal, uniform stress range at the crack. F_s is the correction factor associated with a free surface at the crack origin (the front free surface) while F_w (the back surface or finite width correction) accounts for a free surface at some finite but non-zero crack length. F_e adjusts for the shape of the crack front which is often assumed to be elliptical with minor semidiameter a and major semidiameter b.

F_g is the stress gradient correction factor which accounts for either a nonuniform applied stress (such as bending) or stress concentration caused by detail geometry. This stress gradient should not be confused with that which occurs at the crack tip. F_g represents a more global condition than the crack tip, but may account for a local stress distribution which is not acknowledged by a strength of materials analysis. F_g is directly linked to the choice of S_r and can be a constant in certain instances.

Three methods are currently available for evaluating F_g for varying crack size; all involve finite element (F.E.) analysis. A common technique is the compliance method whereby stress intensity is related to the change in detail compliance with varying crack depth. A second approach is the use of elements with inverse square root singularity. Stress and displacement near the crack tip are related to stress intensity which, therefore, can be output directly from the analysis.

Each of the above methods is expensive since a separate analysis must be made for each crack depth. Also, neither method leads to F_g directly. The other correction factors must be accurately defined if F_g is to be revealed.

The third method of determining F_g is the Green's function or superposition approach.[12,13,16,19,20] Bueckner and Hayes have shown that K for any crack length can be found from the stresses in the crack free body which act upon the plane where the crack forms.[4,10] The advantage of this approach is that only one stress analysis needs to be made for each joint geometry. This advantage makes the third method particularly attractive in any parametric study.

The objectives of this investigation were:

1. To determine F_g for transverse stiffeners fillet-welded to flanges and cover plates with transverse end welds.
2. To develop a technique for predicting F_g automatically for a variable detail geometry.

In each detail analyzed, F_g has been evaluated through use of a Green's function suggested by Albrecht and Yamada.[1]

N. ZETTLEMOYER is Research Engineer, Exxon Production Research Co., Houston, Texas; J. W. FISHER is Professor of Civil Engineering and Associate Director, Fritz Engineering Laboratory, Lehigh University, Bethlehem, Pennsylvania.

Crack Free Stress Analyses

Analytical Models

The overall detail geometries for the stiffener and cover plate investigations are shown in Figs. 1 and 2, respectively. In both cases the detail was assumed to exist on both sides of the beam web which, therefore, marks a plane of symmetry. The midlength of each detail also marks a plane of symmetry. Uniform stress was input to the details at a position far enough removed from the fillet weld so as to exceed the limit of stress concentration effects. In both details the flange width was held constant. The fillet weld angle was set at 45 deg.

The thickness of a stiffener is generally small compared to the flange thickness T_f. Hence, the stiffener itself was omitted from Fig. 1. The variable under investigation was the weld leg Z. Z can be expected to range between 0.25 T_f and 1.00 T_f. The three values of Z selected for this study were 0.32 T_f, 0.64 T_f, and 0.96 T_f. A stress concentration analysis was completed for each value.

A pilot study on the cover-plated detail (Fig. 2) revealed that stress concentration reaches a plateau with increasing attachment length. Hence, the length of cover plate was set so as to ensure maximum concentration conditions. The width of cover plate was held constant and the weld size was assumed constant along the cover plate edge. The variables studied were the weld leg Z, and cover plate thickness T_{cp}. The weld leg sizes considered

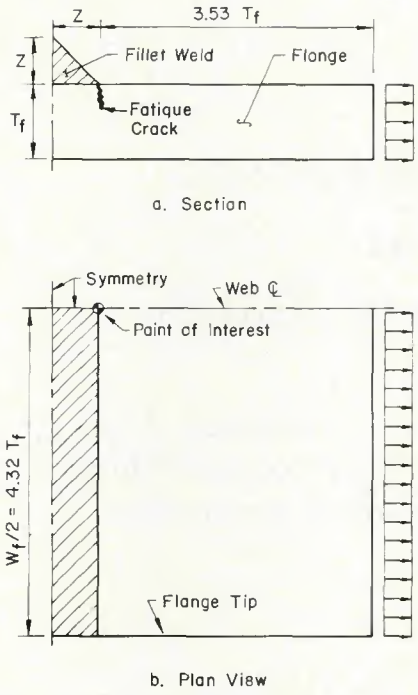

Fig. 1—Detail geometry for transverse stiffener investigation

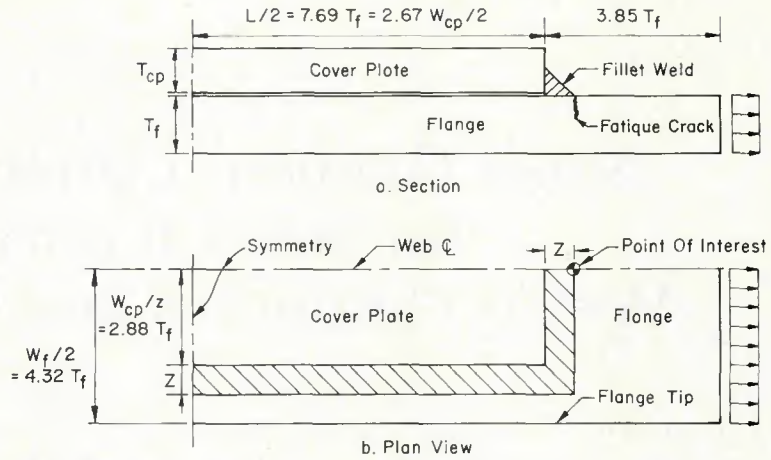

Fig. 2—Detail geometry for cover plate investigation

were the same as for the stiffener detail and the cover plate thickness was taken as 0.64 T_f, 1.44 T_f, and 2.00 T_f.

Both of the details were initially analyzed three-dimensionally. To reduce costs, however, this first level of investigation was only of sufficient accuracy to provide reasonable input to a more local, two-dimensional stress analysis. For the two details studied, fatigue cracks normally originate along the weld toe and propagate through the flange thickness.[6-8] Hence, the plane of interest for two-dimensional stress analysis was the section shown in Figs. 1 and 2. Pilot studies showed that the stress concentration increases slightly as the section gets nearer the web line. Therefore, the specific section for two-dimensional analysis was taken right at the web line.

An existing finite element computer program, SAP IV,[2] was used for the entire stress analysis effort. The program is intended for elastic analysis only; Young's modulus was set at 29,600 ksi (2×10^5 MPa) and Poisson's ratio was taken to be 0.30. A three-dimensional coarse mesh, using brick elements, was established for each detail and subjected to uniform stress. Nodal displacement output from the 3D mesh was then input to a two-dimensional fine mesh. Nodal displacement output from the fine mesh was subsequently input to an ultra fine mesh which was very local to the weld toe. Finally, the element stress concentrations were extrapolated to give a maximum stress concentration factor, SCF, right at the weld toe.

Figures 3 and 4 show the coarse meshes used for each detail. The dashed lines are intended to indicate how the variable cover plate thickness and/or weld leg dimension were effected. In all cases the flange discretization and actual thickness (0.78 in., i.e., 19.8 mm) were held constant. Also, the first line of weld elements adjacent to the overall weld toe had constant size. For both models, displacements perpendicular to lines of symmetry were prevented. Displacement perpendicular to each plan view was prevented along the web line and, in the stiffener case, also along the weld line of symmetry (to simulate the stiffener).

Figures 5 and 6 show the fine and ultra fine meshes which were common to both detail investigations. Planar elements of constant thickness were used throughout. The heavy lines denote the outline of previous mesh elements. Displacements at common mesh nodes along the border were known from the prior analysis; displacements at newly created nodes at the boundary were found by linear interpolation between known values.

The need for an ultra fine mesh deserves further explanation. The assumed geometry at the weld toe creates an elastic stress singularity condition. Hence, a decrease in mesh size adjacent to the toe yields ever higher stress values. However, the

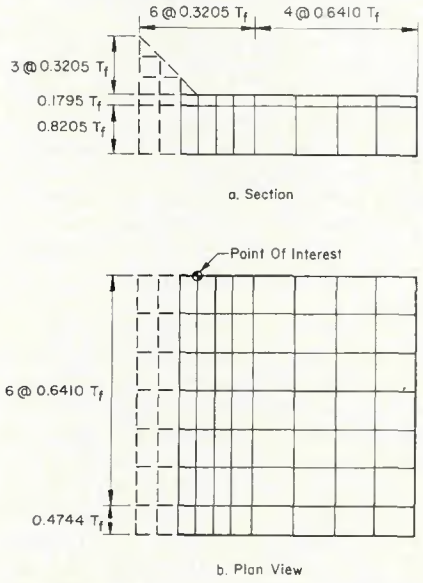

Fig. 3—Coarse mesh for transverse stiffener investigation

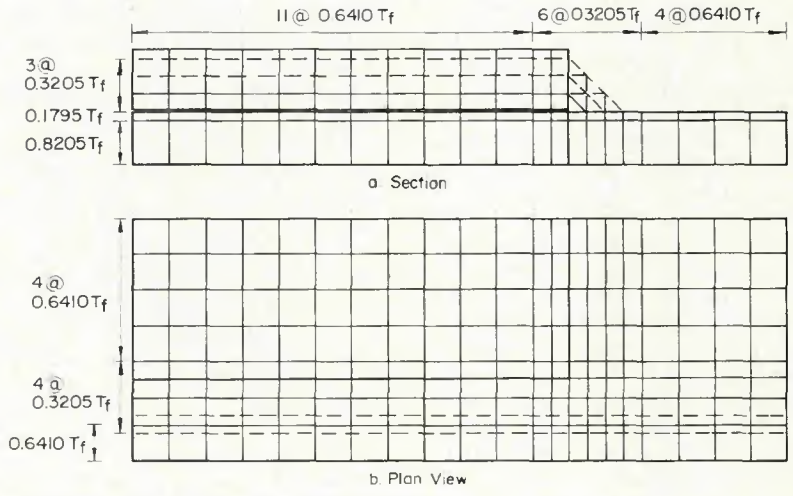

Fig. 4—Coarse mesh for cover plate investigation

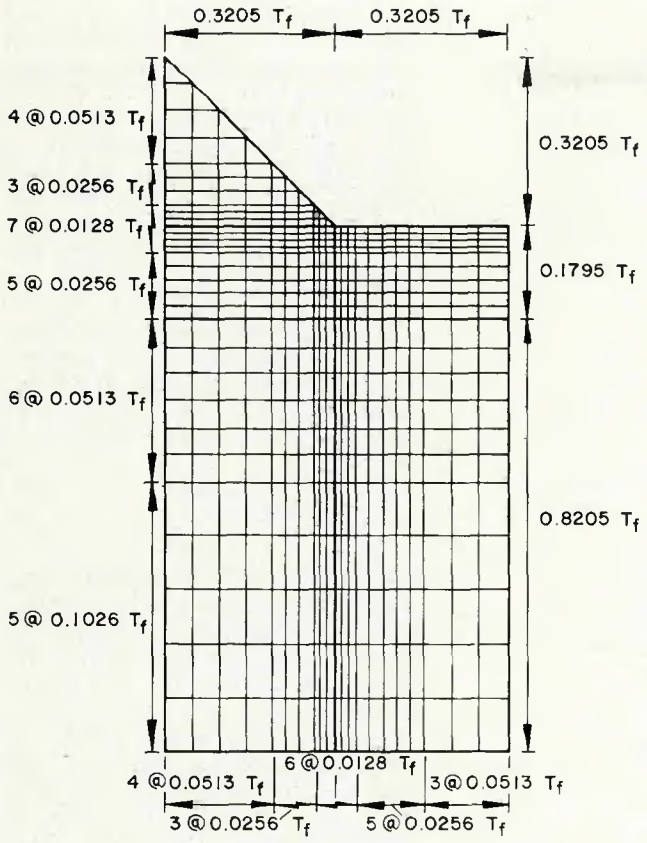

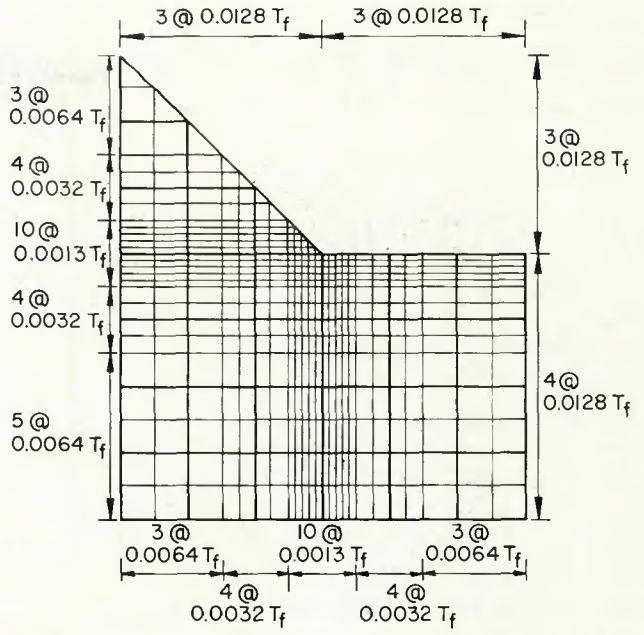

Fig. 6—Ultra fine mesh for stiffener and cover plate investigations

Fig. 5 (left)—Fine mesh for stiffener and cover plate investigations

stresses somewhat removed from the toe become stabilized and the distance to stabilization decreases with decreasing mesh size.

Since the analyst is interested in accuracy of stresses beyond the initial crack size, it seemed reasonable to ensure the mesh size was at least as small as the initial crack size. For the assumed flange thickness (0.78 in. or 19.8 mm), the minimum mesh size was 0.001 in. (0.025 mm). Several investigations have established this as a lower limit of initial crack size.[18,21]

A hypothetical maximum stress concentration factor was obtained by fitting a fourth order polynomial through the averaged concentration values for elements on either side of the node line down from the weld toe in the ultra fine mesh.

Stress Concentration Results

The SCF values for each stiffener and cover plate geometry analyzed are plotted in Fig. 7. SCF increases for increasing stiffener weld size, but decreases for increasing cover plate weld size. These trends are similar to Gurney's findings for non-load-carrying and load-carrying cruciform joints.[9] Apparently, a transition from a non-load-carrying to load-carrying condition occurs as the attachment length along the beam increases.

Regression analyses for the stiffener and cover plate data suggest the following equations:

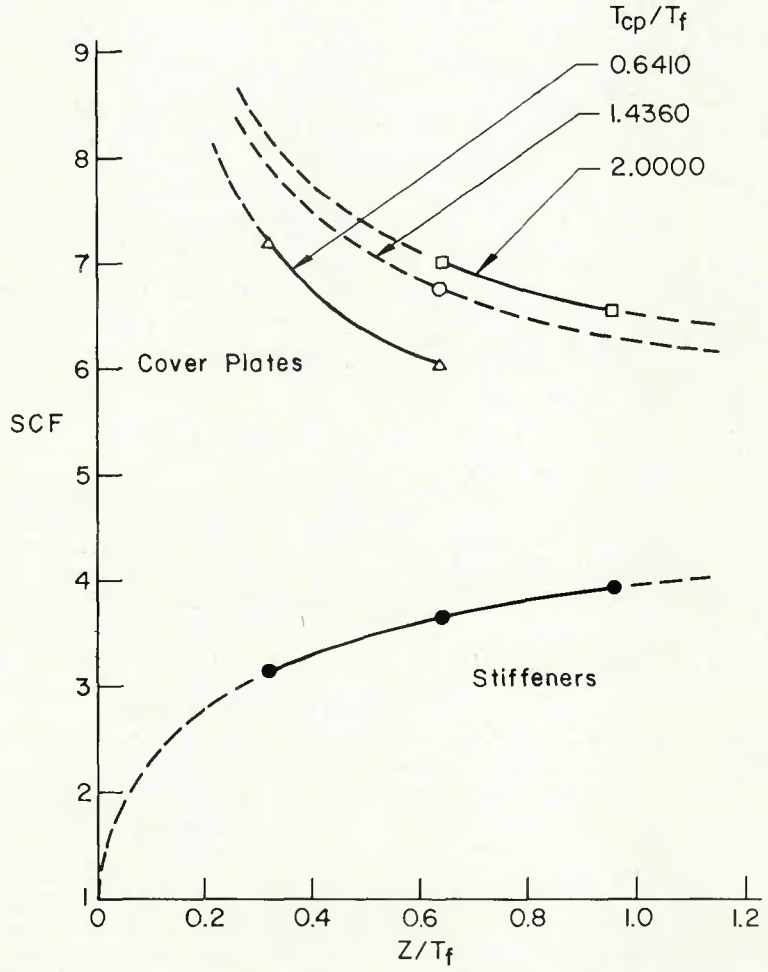

Fig. 7—Variation of maximum stress concentration factor with weld size at stiffener and cover plate details

Stiffeners:

$$SCF = 1.621 \log \left(\frac{Z}{T_f} \right) + 3.963 \quad (2)$$

Cover Plates:

$$SCF = -3.539 \log \left(\frac{Z}{T_f} \right) + 1.981 \log \left(\frac{T_{cp}}{T_f} \right) + 5.798 \quad (3)$$

The standard errors of estimate s for eqs. 2 and 3 are 0.0019 and 0.0922, respectively.

Stress concentration factor decay curves for sample stiffener and cover plate details are plotted in Fig. 8. Each K_t curve eventually drops below 1.0 due to the equilibrium requirement. The cover plate is seen to cause much more disruption to stress flow than does the stiffener. In both cases the stress concentration is most pronounced at small crack sizes. Unfortunately, most of the fatigue life is expended in the same range.[5]

Stress Gradient Correction Factor

Green's Function

The Green's function or superposition approach makes use of stress intensity solutions for loading directly on the crack surface. Use of the Green's function suggested by Albrecht and Yamada leads to the following stress intensity expression:[1]

$$K = \sigma \sqrt{\pi a} \frac{2}{\pi} \int_0^a \frac{K_t}{\sqrt{a^2 - l^2}} dl \quad (4)$$

where σ is the nominal stress on the section and K_t is the crack free stress concentration factor at position l. Since $\sigma\sqrt{\pi a}$ is the stress intensity for a through crack under uniform stress, the stress gradient correction factor, F_g, at crack length a is:

$$F_g = \frac{2}{\pi} \int_0^a \frac{K_t}{\sqrt{a^2 - l^2}} dl \quad (5)$$

If the crack length, a, and distance, l, are both nondimensionalized by the flange thickness, T_f, eq. 5 becomes:

$$F_g = \frac{2}{\pi} \int_0^\alpha \frac{K_t}{\sqrt{\alpha^2 - \lambda^2}} d\lambda \quad (6)$$

where $\alpha = a/T_f$ and $\lambda = l/T_f$

Occasionally, it is possible to express K_t by a polynomial equation such as:

$$\frac{K_t}{SCF} = 1 + A\lambda + B\lambda^2 + C\lambda^3 + D\lambda^4 \quad (7)$$

where A, B, C, and D are dimensionless constants. For such a representation of stress concentration, eq. 6 can be solved in a closed-form manner:

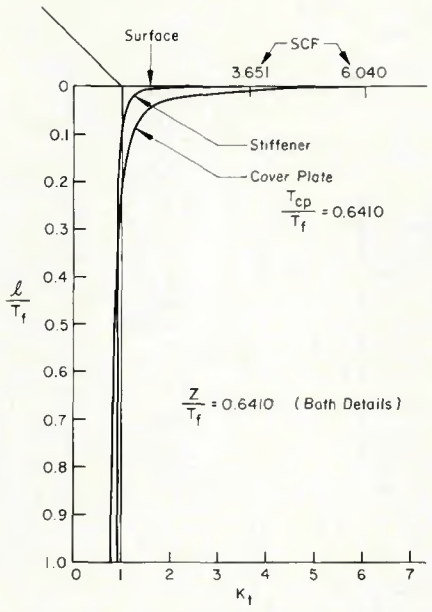

Fig. 8—Stress concentration factor decay from weld toe through flange thickness at sample stiffener and cover plate details

$$\frac{F_g}{SCF} = 1 + \frac{2A}{\pi}\alpha + \frac{B}{2}\alpha^2 + \frac{4C}{3\pi}\alpha^3 + \frac{3D}{8}\alpha^4 \quad (8)$$

Equation 8 can be applied to polynomials of lesser order by merely equating the appropriate decay constants to zero.

It is difficult to make use of eq. 8 for stiffeners and cover plates since the typical concentration curves (Fig. 8) are not well suited to polynomial representation. Hence, eq. 5 usually cannot be solved in a closed-form manner. However, a numerical solution is easily devised as suggested by Albrecht:[1]

$$F_g = \frac{2}{\pi} \sum_{j=1}^{m} K_{tj} \left[\arcsin \left(\frac{l_{j+1}}{a} \right) - \arcsin \left(\frac{l_j}{a} \right) \right] \quad (9)$$

in which K_{tj} is the stress concentration factor in element j of the finite element discretization or the average of two adjacent elements, both of equal distance along opposite sides of the crack path. Limit m is the number of elements to crack length a.

Correction Factor Results

Figure 9 shows the predicted trend of the stress gradient correction in relation to stress concentration at typical welded details. Both the F_g and K_t curves begin at SCF. Each decays to a level below 1.0 although the F_g decay is less rapid. In general, the separation of the two curves at any point other than the origin depends on detail geometry.

Figure 10 presents F_g decay curves (F_g/SCF) for sample stiffener and cover plate details. Usually, the curves for cover plates are below those for stiffeners since the SCF values are higher. It is also apparent that details with similar SCF often have different decay rates. This fact means that the F_g curve is related to a different mix of geometrical parameters than is SCF.

Correction Factor Prediction

It is highly advantageous to have a means of obtaining F_g for different details without individual finite element studies. One approximate method is to represent the F_g equation as:

$$\frac{F_g}{SCF} = \frac{1}{1 + \frac{1}{d}\alpha^q} \quad (10)$$

For a typical stiffener geometry constants d and q can be taken as 0.3602 and 0.2487, respectively. An average cover plate detail is reasonably represented by values of 0.1473 and 0.4348.

A second, more precise method of obtaining F_g is also available. It can be seen that the characteristics of the F_g curve (Fig. 9) are quite similar to features of stress concentration decay (based on gross section stress) from the end of an elliptical hole in an infinite, uniaxially stressed plate.[3,15] Each curve begins at the maximum concentration factor, SCF, and decays to a value near one. (The asymptote for the elliptical hole is exactly 1.) Therefore, it is possible to correlate a hypothetical hole to actual F_g curves (Fig. 10) such that any F_g curve can be estimated from the appropriate hole shape and size.

The elliptical hole shape determines the maximum stress concentration factor:

$$SCF = 1 + 2\frac{g}{h} \quad (11)$$

in which g and h are the hole major and minor semidiameters, respectively. Conversely, given the maximum concentration at a detail (eqs. 2 and 3), the correlated hole shape can be determined.

Figure 11 shows the stress concentration factor decay from an elliptical hole is dependent on both the hole shape and its absolute size. A smaller hole has a more rapid concentration decay. In order to predict F_g from the elliptical hole K_t curve, it is necessary to establish the proper ellipse size—semidiameter g. Such correlation is here based on equal life prediction for crack growth through the flange thickness.

Stress concentration decay along the major axis of an elliptical hole (uniaxial tension in minor axis direction) can be expressed as:[3]

$$K_t = \left[\frac{1}{8} \left\{ 1\text{-}2e^{2\gamma} + e^{4\gamma} \right\} \left\{ 3\text{-}4e^{-2n} + e^{-4n} \right\} \right.$$

$$- \frac{1}{8} e^{4(\gamma - n)} + \sinh(2n) \left\{ \cosh(2n) + \right.$$

$$\left. \left. \frac{1}{2} \cosh(2\gamma) - \frac{3}{2} \right\} \right] /$$

$$\left(\cosh(2n) - 1 \right)^2 \qquad (12)$$

in which n is the general elliptic coordinate and γ is the specific value of n associated with the hole perimeter. The elliptic coordinate can readily be evaluated.

$$\cosh(\gamma) = \left[\frac{1}{1 - \left(\frac{h}{g} \right)^2} \right]^{1/2} \qquad (13)$$

$$\cosh(n) = \left\{ 1 + \frac{a}{g} \right\} \cosh(\gamma) \qquad (14)$$

For any given geometry and assumed value of crack length, a, the stress concentration factor K_t is known if g is known. Further, if g has been correlated to equate K_t and F_g, then the stress gradient correction factor is also established.

A correlation study for the geometries investigated related the optimum ellipse size to the various geometrical parameters and initial crack size a_i. The regression curves which resulted are:

Stiffeners:

$$\frac{g}{T_f} = -0.002755 + 0.1103 \left(\frac{Z}{T_f} \right) - 0.02580 \left(\frac{Z}{T_f} \right)^2 + 0.6305 \left(\frac{a_i}{T_f} \right) - 7.165 \left(\frac{a_i}{T_f} \right)^2 \qquad (15)$$

Cover Plates:

$$\frac{g}{T_f} = 0.2679 + 0.07530 \left(\frac{Z}{T_f} \right) - 0.08013 \left(\frac{Z}{T_f} \right)^2 + 0.2002 \log \left(\frac{T_{cp}}{T_f} \right) + 1.391 \left(\frac{a_i}{T_f} \right) - 11.74 \left(\frac{a_i}{T_f} \right)^2 \qquad (16)$$

The standard errors of estimate s for eqs. 15 and 16 are 0.0041 and 0.0055, respectively.

Figure 12 compares the K_t curve at a sample cover plate detail with the actual F_g curve from the Green's function (eq. 9) and the F_g curve from the correlated ellipse. It is apparent the two F_g curves are in close agreement and cross over each other twice. Such is also common for stiffener details.

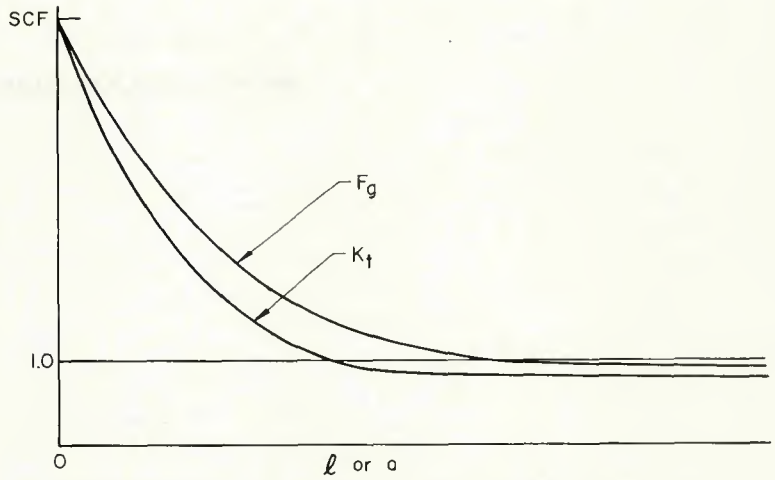

Fig. 9—Schematic stress concentration and stress gradient correction factor decay curves for typical welded details

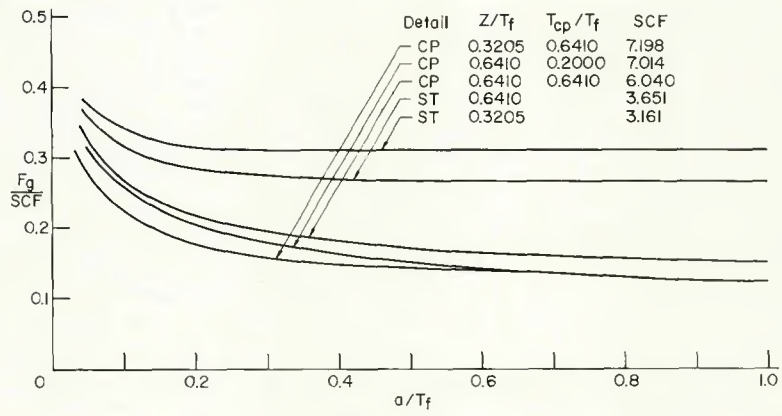

Fig. 10—F_g decay curves for sample stiffener and cover plate details

Conclusion

Stress concentration analyses have been conducted for stiffener and cover plate welded details. The resulting stress gradients have been transformed into a correction factor for stress intensity through use of an appropriate Green's function.

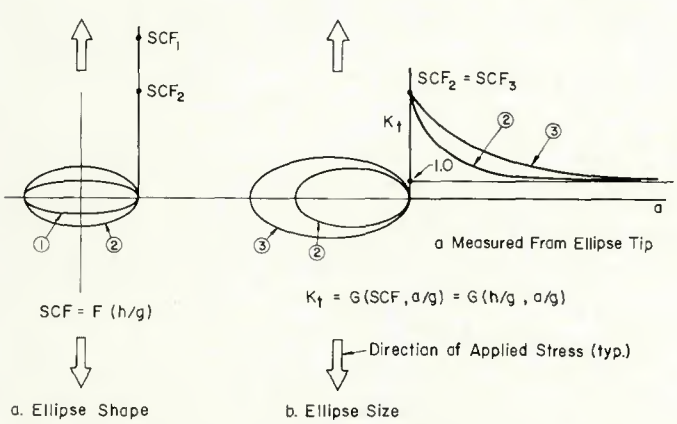

Fig. 11—Two steps required for ellipse correlation

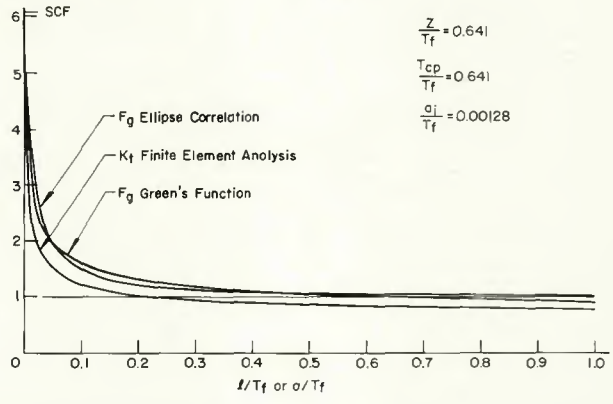

Fig. 12—Comparison of K_t and F_g decay curves for sample cover plate detail

The correction factor curves were correlated with stress concentration factor decay from an elliptical hole in a uniaxially stressed plate. Such correlation has provided a means of predicting the correction factor for arbitrary geometries.

Automatic prediction is necessary for rapid fatigue analysis of these typical details.

References

1. Albrecht, P., and Yamada, K., "Rapid Calculation of Stress Intensity Factors," *Journal of the Structural Division*, ASCE, Vol. 103, No. ST2, Proc. Paper 12742, February 1977, pp. 377-389.
2. Bathe, K. J., Wilson, E. L., and Peterson, F. E., "SAP IV—A Structural Analysis Program for Static and Dynamic Response of Linear Systems," Earthquake Engineering Research Center Report No. EERC 73-11, University of California, Berkeley, California, June 1973 (revised April 1974).
3. Biezeno, C. B., and Grammel, R., "Elastic Problems of Single Machine Elements," Vol. II, *Engineering Dynamics*, Blackie & Son, Ltd., London, England, 1956, pp. 84-90.
4. Bueckner, H. F., "The Propagation of Cracks and the Energy of Elastic Deformation," *Transactions*, American Society of Mechanical Engineers, Vol. 80, 1958, p. 1225.
5. Fisher, J. W., Frank, K. H., Hirt, M. A., and McNamee, B. M., "Effect of Weldments on the Fatigue Strength of Steel Beams," NCHRP Report No. 102, Highway Research Board, National Academy of Sciences—National Research Council, Washington, D. C., 1970.
6. Fisher, J. W., Albrecht, P. A., Yen, B. T., Klingerman, D. J., and McNamee, B. M., "Fatigue Strength of Steel Beams with Welded Stiffeners and Attachments," NCHRP Report No. 147, Transportation Research Board, National Research Council, Washington, D. C., 1974.
7. Frank, K. H., "The Fatigue Strength of Fillet Welded Connections," Ph.D. Dissertation, Lehigh University, Bethlehem, Pa., October 1971.
8. Gurney, T. R., *Fatigue of Welded Structures*, Cambridge University Press, London, England, 1968.
9. Gurney, T. R., "Finite Element Analyses of Some Joints with the Welds Transverse to the Direction of Stress," *Welding Research International*, Vol. 6, No. 4, 1976.
10. Hayes, D. J., "A Practical Application of Bueckner's Formulation for Determining Stress Intensity Factors for Cracked Bodies," *International Journal of Fracture Mechanics*, Vol. 8, No. 2, June 1972, p. 157.
11. Irwin, G. R., "Analysis of Stresses and Strains Near the End of a Crack Traversing a Plate," *Transactions*, American Society of Mechanical Engineers, Series E, Vol. 79, September 1957, p. 361.
12. Kobayashi, A. S., "A Simple Procedure for Estimating Stress Intensity Factor in Region of High Stress Gradient," *Significance of Defects in Welded Structures*, Proceedings, 1973 Japan-U.S. Seminar, University of Tokyo Press, Tokyo, Japan, 1974, p. 127.
13. Lawrence, F. V., "Estimation of Fatigue-Crack Propagation Life in Butt Welds," *Welding Journal*, 52 (5), May 1973, Research Suppl., pp. 212-s to 220-s.
14. Maddox, S. J., "Assessing the Significance of Flaws in Welds Subject to Fatigue," *Welding Journal*, 53 (9), September 1974, Research Suppl., pp. 401-s to 409-s.
15. Neuber, H., *Kerbspannungslehre*, 2nd ed., Springer-Verlag, Berlin, Germany, 1958, pp. 52-56.
16. Paris, P. C., and Sih, G. C., "Stress Analysis of Cracks," Fracture Toughness Testing and Its Applications, STP 381, American Society for Testing and Materials, Philadelphia, Pa., 1965, p. 30.
17. Randall, P. N., "Severity of Natural Flaws as Fracture Origins, and a Study of the Surface-Cracked Specimen," AFML-TR-66-204, August 1966 (published in ASTM STP 410, p. 88).
18. Signes, E. G., Baker, R. G., Harrison, J. D., and Burdekin, F. M., "Factors Affecting the Fatigue Strength of Welded High Strength Steels," *British Welding Journal*, Vol. 14, No. 3, March 1967, p. 108.
19. Tada, H., Paris, P. C., and Irwin, G. R., *The Stress Analysis of Cracks Handbook*," Del Research Corporation, Hellertown, Pa., 1973.
20. Tada, H., and Irwin, G. R., "K-Value Analysis for Cracks in Bridge Structures," Fritz Engineering Laboratory Report No. 399.1, Lehigh University, Bethlehem, Pa., June 1975.
21. Watkinson, F., Bodger, P. H., and Harrison, J. D., "The Fatigue Strength of Welded Joints in High Strength Steels and Methods for its Improvement," *Proceedings*, Fatigue of Welded Structures Conference, Welding Institute, Brighton, England, 1971.

Appendix: Notation

The following symbols are used in this paper:

- a = crack size
- a_i = initial crack size
- A = stress concentration factor decay polynomial coefficient
- B = stress concentration factor decay polynomial coefficient
- C = stress concentration factor decay polynomial coefficient
- d = stress gradient correction factor decay coefficient
- D = stress concentration factor decay polynomial coefficient
- F_e = crack shape correction factor
- F_g = stress gradient correction factor
- F_s = front free surface correction factor
- F_w = back free surface correction factor
- g = major semidiameter of elliptical hole in an infinite plate
- h = minor semidiameter of elliptical hole in an infinite plate
- ΔK = range of stress intensity factor
- K_t = stress concentration factor
- l = distance along crack path from origin
- L = cover plate length
- log = logarithm to base 10
- m = number of finite elements to crack length a
- q = stress gradient correction factor decay exponent
- s = standard error of estimate
- S_r = stress range
- SCF = maximum stress concentration factor at crack origin
- T_{cp} = cover plate thickness
- T_f = flange thickness
- W_{cp} = cover plate width
- W_f = flange width
- Z = weld leg size
- α = nondimensionalized crack length, a/T_f
- γ = value of elliptic coordinate n representing elliptical hole perimeter
- n = elliptic coordinate
- λ = nondimensionalized distance, l/T_f
- σ = nominal stress